

International Council for the
Exploration of the Sea

C.M. 1980 / C : 12
Hydrography Committee



Statistical model of meso-scale temperature and current
fluctuations over the Iceland-Faroe Ridge slope

by

Jürgen Willebrand and Jens Meincke

Institut für Meereskunde, Düsternbrooker Weg 20, 2300 Kiel, F.R. Germany

Introduction

The submarine ridge system between Greenland and Scotland constitutes a major obstacle for the spreading of the cold (-0.5 to -0.9° C) and relatively saline ($\approx 34.92^{\circ}/\text{oo}$) water from its formation area in the Greenland/Norwegian Seas into the North Atlantic. Ever since KNUDSEN (1899) first observed this overflow, numerous field studies were aimed at determining the scales of its variations in space and time. Whereas the topographic control of the overflow process and the spatial scales of its fluctuations could be determined on the basis of sufficiently dense hydrographic sections or even synoptic surveys that became available until 1960, (for references see HANSEN and MEINCKE, 1979) it was not until 1973 that continuous records of 30 to 50 days duration were obtained from moored instruments deployed during the expedition "Overflow '73" (ICES 1975). From these data MEINCKE (1975) and ROSS (1976) suspected that overflow-events were correlated with changes of the atmospheric pressure distribution at the synoptic scale of order 10 days.

In order to obtain statistically significant information on the time scale of overflow-variations, the joint USA/Iceland/UK/USSR and F.R. Germany project MONA (Monitoring the Overflow into the North Atlantic) was launched in 1975 by mooring near bottom current meters at 7 positions on the Greenland-Scotland ridge. In the Denmark-Strait the by far largest signal in the low frequency band was observed at a time scale of 1.5 to 2.5 days with

amplitudes comparable to the mean flow (AAGAARD and MALMBERG, 1978). The authors contribute this to a baroclinic instability process with the statistics however being highly non-stationary. A preliminary analysis of time series on the Iceland-Faroe ridge and in the Faroe-Shetland Channel (MEINCKE and KVINGE, 1978) occasionally indicated energy maxima in the period bands 8 to 11 days and 2 to 5 days in correspondence to spectra of atmospheric pressure. However, coherences between the variables were mostly below marginal and no interpretation was possible in terms of direct coupling between atmospheric and oceanographic fluctuations. Continuing with the analysis of these data, the present paper investigates the spectral properties of the recorded oceanographic parameters for the period range from 2 hours to about 50 days. It is the aim to describe the relation between the observed fluctuations and the regional hydrography and to discuss the effectiveness of baroclinic instabilities versus meteorological forcing in causing the fluctuations.

The hydrographical setting

Figure 1 shows the topography of the southeastern portion of the Iceland-Faroe ridge and most of the Faroe-Shetland channel which are both part of the Greenland-Scotland ridge system. Whereas the northeastern flank of the Iceland-Faroe ridge has a uniform slope with the isobaths in southeast-northwest direction, the crest is characterized by a series of notches cutting across (FLEISCHER et al., 1975). Figure 1 shows that the mooring MONA 3 is located in the transition area between one of the notches and the flank with the local isobaths (at 5 km scale) in east-west direction. This is in contrast to the location of mooring MONA 1 which was moored in the deep and narrowing part of the Faroe-Shetland channel in smooth topography with the isobaths in northeast-southwest direction. Table 1 gives the exact positions of the moored instruments and other relevant information. The contrast in topographic conditions for MONA 1 and 3 also holds for the hydrographic situation. Figure 2 shows the characteristic distribution of temperature on sections past the

mooring location. It clearly locates the instrument on MONA 3 into the zone of the polar front which parallels the southeastern part of the Iceland-Faroe ridge (HANSEN and MEINCKE, 1979). The typical width of the front near the bottom is 30 km and it separates the nearly homogeneous Norwegian Sea deep water from the stratified mixed waters on the Atlantic side of the front (MEINCKE, 1978). Meandering and eddying in the frontal zone at spatial scales of the order 30-50 km locally leads to temperature changes as demonstrated in Figure 3. During phases of higher ambient temperature the amplitudes of shorter term (tidal) fluctuations are high, whereas the presence of Norwegian Sea deep water leads to the low temperature cut-off around -0.5° C with only very small fluctuations, despite unchanged amplitudes of the tidal currents.

In contrast to the conditions at MONA 3 the instrument on MONA 1 was permanently located in Norwegian Sea deep water. Although the temperature sensor failed this statement is safe since more than 50 years of monitoring the Faroe-Shetland channel have proven the persistence of the nearly homogeneous deep water at these depths (MARTIN, 1966).

Kinematical structure of current fluctuations

Frequency spectra of twice the horizontal kinetic energy (HKE) at stations MONA 1 and MONA 3 are shown in figure 4. The spectra are dominated by a strong peak at 2 cpd. The frequency resolution is such that inertial oscillations and semidiurnal tides are not resolved. A further peak occurs at 1 cpd and indicates a diurnal component which is dominated by the O_1 -tide (KOLTERMANN, 1978). Outside this frequency range the spectra decrease smoothly and approximately proportional to a ω^{-2} power-law. At long periods (> 10 d) the spectra become more or less flat. An energy-conserving plot (not shown) would have a peak around 10 days.

Both the spectra at MONA 1 and MONA 3 are rather similar in shape but not in magnitude. Throughout the low-frequency range, the values at MONA 3 exceed those at MONA 1 by a factor of 2-3 while at high frequencies the energies are identical. That factor is close to the square of the depth ratio $(H_1/H_3)^2 \approx 3.1$. As low-

frequency current fluctuations in the area are normally nearly barotropic (KOLTERMANN et al., 1976), we conclude that within their statistical accuracy the low-frequency mass transport fluctuations at both stations are almost identical.

In order to investigate the horizontal scales of motion, we have calculated cross-spectra between various current components at MONA 1 and MONA 3. As an example in figure 5 coherence and phase between the NE-components at both stations is shown. These curves are representative for all other combinations of components. Generally, the coherences are rather low. Only at semi-diurnal and diurnal periods significant values were found between all components. At low frequencies few coherence values are marginally significant, e.g. at 6.6 days period. If that coherence is not spurious it would indicate propagation of a signal between MONA 1 and MONA 3 (the component at MONA 3 leads). We feel, however, that conclusions about wavelengths and propagation direction based on a single marginal coherence would be rather shaky. Further and more closely spaced stations are required to determine the horizontal scales of motion uniquely from current measurements alone.

The following analysis of the current fluctuations is performed in a rotary rather than cartesian representation of the current vector (GONELLA, 1972). The argument for this choice is that the surrounding topography is extremely irregular and no "natural" coordinate system can be identified easily. We will consider energy spectra (E) of the clockwise (+) and anticlockwise horizontal velocity components. A useful number is the ratio $E_+(\omega)/E_-(\omega)$ which contains information on the kinematical structure of the motion. (The sum of both quantities is, of course, identical to the HKE plotted in figure 4). The simplest conceivable situation would be described by linear, inviscid and unforced dynamics, with the horizontal momentum balance given by

$$(1) \quad \frac{\partial \mathbf{u}}{\partial t} + \mathbf{f} \times \mathbf{u} = - \frac{1}{\rho_0} \Delta p$$

in standard notation. Assuming a superposition of plane waves with random phase relations, one can derive from (1) the consistency relation

$$(2) \quad \frac{E_+(\omega)}{E_-(\omega)} = \frac{(f - \omega)^2}{(f + \omega)^2}$$

(MÜLLER and SIEDLER, 1976).

The observed values E_+/E_- from stations MONA 1 and MONA 3 are plotted in figure 6. Also shown is the theoretical curve (2) (full line). With few exceptions, the observed values are larger than prediction (2) and show an excess of counter-clockwise energy, or more precisely a lack of excess of clockwise energy. Only around 10 days at station MONA 1 there is an opposite tendency, with too much clockwise energy.

As the violations of relation (2) are significant at the 95 % level, we have to ask for possible mechanisms causing this behaviour. One possible candidate is friction as both current meters are close to the bottom and may be affected by turbulence in a frictional layer. Considering a simple Guldberg-Mohn friction in (1) the consistency relation becomes

$$(3) \quad \frac{E_+(\omega)}{E_-(\omega)} = \frac{(f - \omega)^2 + \lambda^2}{(f + \omega)^2 + \lambda^2}$$

where λ^{-1} is an effective dissipation time. The dashed line in figure 6 corresponds to (3) with a constant value $\lambda^{-1} = 1.5$ h. At MONA 3 eq. (3) is a much better description of the observations than the frictionless form (2), except near tidal and inertial frequencies. The discrepancies could be further reduced by relaxing the physical unreasonable assumption that λ is constant with frequency. Therefore we conclude that at MONA 3 the current fluctuations are consistent with a description by randomly superposed free waves with friction invoked.

The situation at MONA 1 is somewhat different. First of all, at high frequencies the observed values of E_+/E_- exceed those at MONA 3 and hence would require a larger value for the frictional "constant". This would be surprising as the instrument at MONA 1 is located 51 m above the bottom as compared to 17 m at MONA 3 so

that one would expect stronger frictional influence at MONA 3. Furthermore, some values of E_+/E_- are outside the range which in principle can be reached by (3), namely exceeding unity (especially at diurnal period) and below the theoretical curve (2) (around 10 days). Thus it seems that friction alone cannot explain the observations at MONA 1. It is more likely that the complicated channel geometry imposes constraints on the phases of different wavetrains. In this case the theoretical ratio E_+/E_- depends on these phase differences, and no simple results as (2) or (3) are available.

In order to obtain information on the directional structure of the fluctuations we consider the coherence γ_{+-} between the two rotary components. Perfect coherence is equivalent to a unique orientation Ψ of the current ellipse which is related to the phase difference ϕ_{+-} by $\Psi = \phi_{+-}/2$ (Ψ counted mathematically positive from east). Perfect coherence generally indicates a monochromatic wave train in the horizontal plane. Zero coherence, on the other hand, implies that the current ellipse degrades into a circle and that there is no preferred direction of principal axes, although this does not necessarily indicate horizontal isotropy (cf. WILLEBRAND et al., 1977).

Coherence γ_{+-} and phase difference ϕ_{+-} for stations MONA 1 and MONA 3 are shown in figure 8. The coherence is significant nearly everywhere and indicates a strong directionality, at MONA 3 somewhat less than at MONA 1. Especially large values occur at semidiurnal tides. Except for the tides, coherence gradually decreases toward higher frequencies, and the directional distribution becomes more diffuse. Most phases are between 0° and 90° , and the orientation of the current ellipse does not vary much with frequency.

The ratio of major/minor principal axes and their orientation is listed in table 2. The direction of the major principal axis contains information about the horizontal direction of the disturbances. In case that the simple model (1) applies, both directions are identical, and the propagation direction is determined up to $\pm 180^\circ$. It is obvious that these directions

should be related to the topography map (figure 1), especially at low frequencies where the consistency relation (2) is valid. By and large, we find NE-SW direction at MONA 1, and E-W direction at MONA 3, parallel to the bottom contours. Thus, it seems that the fluctuating motion is strongly controlled by the local topography.

Temperature measurements analysis

The temperature time series obtained at position MONA 3 has a mean value of 0.7° C and a rms derivation of 1.1° C. As already discussed, the temperature time series in figure 3 shows a markedly non-gaussian distribution with frequent low-temperature cut-offs around -0.5° C, a pattern related to advection of the polar front past the instrument.

The temperature autospectrum is shown in figure 9. The spectrum is rather smooth and decreases with a slope around -2 at frequencies above .1 cpd. The peak at semidiurnal (and inertial) frequency is much less prominent than it is in the current spectrum (fig. 4), and at the diurnal frequency there is no significant peak at all.

The covariance between temperature and current is largest in the direction of 20° clockwise from north with $\langle u'T' \rangle \approx + 2.8^{\circ}$ C cm s^{-1} , a value that significantly differs from zero at the 95 % probability level. The corresponding eddy heat flux into that direction, $H = \rho c_p \langle u'T' \rangle$, is then found to $1,2 \cdot 10^5 \text{ W m}^{-2}$.

Figure 10 shows the cospectrum between temperature and current in 20° vs. frequency in an energy-conserving way such that the area under the curve is proportional to the contribution to the total covariance. It demonstrates that by far the largest contribution to the eddy heat flux comes from periods longer than 10 days.

Figure 11 displays for various periods the coherence between temperature and current as a function of the current direction. At most periods maximum coherence occurs between directions N and NW. We notice that this direction differs by some $30-40^{\circ}$ from the direction of maximum correlation. The cause for that difference

is the strong anisotropic structure of the current fluctuations which have their maximum amplitude in E-W direction.

The coherence between temperature and current in 350° direction is plotted in figure 12 together with the corresponding phase difference. Although the coherence is not very high, it is nevertheless clearly significant at most frequencies. The phase is near zero at low frequencies, indicating that high temperatures and northward currents occur simultaneously. At shorter periods the phase changes towards -90° so that here northward currents precede higher temperatures. It is important to note that this phase shift is significant at the 95 % level despite the low coherence values.

The information in figures 9-12 allows some semi-quantitative conclusions about the heat balance at station MONA 3. The observed correlation between current and temperature suggests that horizontal advection must be a dominant process. WILLEBRAND and MEINCKE (1980) have proposed a stochastic advection model considering the heat balance equation

$$(4) \quad \frac{\partial T}{\partial t} + u_2 \frac{\partial T_m}{\partial x_2} = f - \mu T$$

with $f = -u_\alpha g_\alpha$ (summation over $\alpha = 1, 2$ understood)

where the coordinate system is oriented such, that x_2 is in the direction of 350° which on the average gives the largest coherence between current and temperature. T_m is a local time average of temperature used to define the mean temperature gradient, μT represents the diffusion term and g_α is a fluctuating horizontal temperature gradient. Now if the velocity is a broadband stationary function of time, the fluctuating temperature gradient will be almost independent of the local instantaneous velocity. Hence the forcing term f in (4) is uncorrelated with u and effectively acts as "noise". The spectrum E_f can be found to be

$$(5) \quad E_f(\omega) = \int d\omega' E_{HKE}(\omega') E_g(\omega - \omega')$$

where $E_{HKE} = E_{u_1} + E_{u_2}$ is the spectrum of (twice) the horizontal

kinetic energy.

In order to evaluate (5) we have to specify the temperature gradient spectrum $E_g(\omega)$. One possible idealization is to think of a number of different water masses, each with its own temperature, being advected past the instrument. In this case the time series of temperature gradient consists of a series of spikes and has a white spectrum, $E_g(\omega) = \text{const}$, and the situation is completely analogous to the one-dimensional case considered by PHILLIPS (1971). Indeed, inspection of the temperature time series in figure 3 reveals that at times the temperature is more or less constant over intervals of nearly a week. At other times, however, the instrument lies in a gradient region of varying intensity as one can see from the intensity of tidal fluctuations in the temperature record. The latter situation would correspond to a spectrum $E_g(\omega)$ peaked at low frequencies.

In a crude way the spectrum can be modelled as a linear combination of both limiting cases,

$$(6) \quad E_g(\omega) = F_0 + F_1 \delta(\omega)$$

with the constants F_0, F_1 yet to be determined. If in addition the mean temperature gradient $\partial T_m / \partial x_2$ and the diffusion constant μ are determined, a theoretical estimate for the curves observed in figures 9 and 12 can be obtained. These parameters can be found by applying some kind of fitting procedure. Less than optimal but sufficiently accurate values can, however, already be determined by inspection. From the high-frequency end of the temperature spectrum where the white part of $E_f(\omega)$ dominates the forcing term we find the constant $F_0 \sim 3.5 \cdot 10^{-13} (\text{°C/cm})^2 / \text{cpd}$. From the phase changes near a period of 7 days in figure 10 we find $\mu \sim (2\pi/7 \text{ days}) = 10^{-5} \text{ sec}^{-1}$. Finally, the parameters $\partial T_m / \partial x_2$ and F_1 are related in a somewhat coupled way to the coherences at low frequencies and to the spectral peak at tidal frequency. By means of a non-systematic trial and error method we find $\partial T_m / \partial x_2 = -10^{-6} \text{°C/cm}$ and $F_1 = .3 \cdot 10^{-12} (\text{°C/cm})^2$.

The theoretical curves with those parameter values are shown

in figures 9 and 12 (dashed lines). By and large, the agreement with the observed values is quite satisfactory. Discrepancies occur in the energy spectrum between .1 cpd and 1 cpd where the theoretical spectrum is too large by some 40 %, and in the coherence curve where the theoretical coherence is generally too large at low frequencies. One obvious reason is the oversimplification in (6).

The total variance of the temperature gradient fluctuations were estimated to be $\langle g^2 \rangle^{1/2} = 2.7 \cdot 10^{-6} \text{ }^\circ\text{C/cm}$, more than double the magnitude of the mean gradient. More than 90 % of that variance is associated with the white part of the spectrum. Knowing the variance of both temperature and temperature gradient we can define a typical horizontal scale L of the fluctuating temperature field by

$$(7) L^2 = \langle T^2 \rangle / \langle g^2 \rangle$$

With the numbers given above an equivalent wavelength $2\pi L \approx 25 \text{ km}$ is yielded in agreement with typical eddy dimensions as found by HANSEN and MEINCKE (1979).

Energetics

Two possible mechanisms are most likely to cause the observed current and temperature fluctuations, namely (i) baroclinic instability of the polar front jet and (ii) generation by atmospheric disturbances. Although the information in our data is by far insufficient to apply a quantitative theory of either mechanism, it is possible to roughly estimate their relative importance.

From turbulent heat flux and mean temperature gradient one can calculate a horizontal eddy diffusivity. Neglecting the difference in the directions of both vectors, we define A_H by $\overline{u_2 T'} = - A_H \partial T_m / \partial x_2$. Inserting the numbers given above we find $A_H = + 3 \cdot 10^6 \text{ cm}^2 \text{ s}^{-1}$.

Turbulent heat flux down the mean temperature gradient indicates that energy is flowing from the mean field into the fluctua-

tions. To decide whether or not an instability mechanism can be effective at all, we estimate the rate of energy conversion S from available potential energy of the mean field into eddy energy. We use the simplified equation of state $\rho = \rho_0 (1 - \beta T)$ and the definitions

$$(8) \quad E_{\text{kin}} = \frac{1}{2} \rho_0 (\overline{u_1'^2} + \overline{u_2'^2})$$

$$E_{\text{pot}} = \frac{1}{2} \frac{g \beta^2}{\rho_0} \frac{\overline{T'^2}}{N^2}$$

for eddy kinetic and available potential energy. In the absence of friction, horizontal shear of the mean flow, and pressure work at the boundaries of the volume of fluid under consideration, and assuming a mean temperature gradient in u_2 (\sim north) - direction, the conversion rate is given by

$$(9) \quad S = - \frac{(g\beta)^2}{\rho_0} \frac{\overline{u_2' T'} \partial T_m / \partial x_2}{N^2}$$

(cf. LORENZ, 1967, PEDLOSKY, 1979).

Inserting the values $\overline{u_1'^2} + \overline{u_2'^2} = 225 \text{ (cm/s)}^2$ for the low frequent (period $> 2\text{d}$) current fluctuations, $N = 3 \cdot 10^{-3} \text{ s}^{-1}$ for the Brunt-Väisälä frequency, $\beta \approx 7 \cdot 10^{-5} \text{ }^\circ\text{C}^{-1}$ and the observed heat flux and rms temperature, we obtain

$$E_{\text{kin}} \approx 110 \text{ erg cm}^{-3}$$

$$E_{\text{pot}} \approx 320 \text{ erg cm}^{-3}$$

$$S \approx + 1.5 \cdot 10^{-3} \text{ erg cm}^{-3} \text{ s}^{-1}$$

The total energy is in the same range as typical values found by BRYDEN (1979) in the Drake Passage while the conversion rate is one order of magnitude higher, largely due to the stronger temperature gradient at MONA 3. Hence, the time scale which can be defined from total energy and conversion rate is much shorter than Bryden's values, namely 3-4 days. That time scale is of

same order as the characteristic time scale of the fluctuations indicating that the energy transfer from mean to fluctuating energy must be an important process in the energy balance of the fluctuations.

In order to investigate the possibility of direct atmospheric generation, we have calculated coherences between all observed oceanic variables and sea level pressure and pressure gradient. Essentially, no significant coherence between any oceanic and atmospheric variable was found. However, this result does not necessarily indicate that atmospheric generation is unimportant, as even in idealized cases not much correlation between atmosphere and ocean can be expected (WILLEBRAND et al., 1979).

The flux of mechanical energy from wind into the ocean is calculated as average product of wind stress and surface velocity $\langle \underline{\tau} \cdot \underline{u}_s \rangle$. Assuming that surface and observed near-bottom velocity are of same magnitude and that the energy is distributed uniformly over the water column, we obtain for the local input rate

$$(10) \quad S_{\tau} = \gamma_{\tau u} \tau_{rms} u_{rms} / H$$

Here $\gamma_{\tau u}$ denotes an average correlation between corresponding wind stress and current components. We estimate $\gamma_{\tau u} \approx 0.3$ as a larger value would have been detected in the analysis. Inserting $\tau_{rms} = 2 \text{ dyne cm}^{-2}$, $u_{rms} = 15 \text{ cm s}^{-1}$ and $H = 500 \text{ m}$, we find $S_{\tau} \leq 3 \cdot 10^{-4} \text{ erg cm}^{-3} \text{ s}^{-1}$, almost an order of magnitude smaller than conversion of mean potential energy.

Summary and discussion

Statistical analysis of one-year current and temperature time series has revealed information on the kinematical structure of the flow, and also allows to speculate on the dynamics governing the motion.

The observed current fluctuations have a dominant time scale of 10 days, considerably longer than the value of 2 days observed in Denmark Strait by SMITH (1976) and AAGAARD and MEINCKE (1978).

At low frequencies (including tides) the currents are strongly anisotropic, their major principal axis being roughly parallel to the bottom contours. Towards higher frequencies the anisotropy is less prominent, especially at MONA 3.

A consistency test was performed in order to test the concept of randomly superposed, linear and free waves. At MONA 3, that concept proved useful at periods longer than 2 days. At higher frequencies additional friction and/or forcing is required to balance momentum, with a time scale from a few hours to less than 1 h. At MONA 1, however, that concept is not applicable probably due to the dominating influence of the geometry preventing the random phases in favour of more organized, basin-mode-like motions.

Temperature variations observed at MONA 3 can be explained almost perfectly in terms of a simple stochastic model consisting of three ingredients: horizontal advection of mean temperature field, advection of eddy temperature field and diffusion. Characteristic parameters which can be determined by fitting the model are mean temperature gradient, horizontal eddy scale and a diffusive time scale. The first two of those parameters are in good agreement with hydrographic observations, and their determination from a single instrument demonstrates the additional information gained by relating current and temperature with a simple model.

From the correlation of current and temperature signal, we inferred a local eddy heat flux of $1.2 \cdot 10^5 \text{ W m}^{-2}$ in northerly direction. Taking the regional orientation of the polar front into account, that indicates an influx of heat into the Norwegian Sea normal to the front. If this number is representative for the total frontal zone between Iceland and the Faroes, i.e. for a depth range from 200 m to 500 m over a length of 440 km then the eddy heat flux contributes $1.6 \cdot 10^{13} \text{ W}$ to the heat budget of the Norwegian Sea. This amount is of the same order as $0.9 \cdot 10^{13}$ which is the heat lost from the southwestern Norwegian Sea by advection of low salinity intermediate water along the frontal zone into southeasterly direction (MEINCKE, 1978) and the transport by Norwegian Sea deep water across the

Iceland-Faroe ridge (WORTHINGTON, 1970). Thus, it is demonstrated that heat flux by eddies is at least locally important, although its contribution to the total heat budget of the Norwegian Sea may still be small.

A strong flux of energy from mean available potential to eddy energy suggests that baroclinic instability is a major source of the low-frequency fluctuations. Whether or not, however, the actual mean temperature and current field at MONA 3 is baroclinically unstable, and if so whether or not the dominating period (~ 10 days) of the observed fluctuations coincides with that of the most unstable waves, is an open question. Attempts to relate current observations quantitatively to instability models have been made by SMITH (1976) for the Denmark Strait, and by MYSAK and SCHOTT (1977) and BRYDEN (1979) for other areas. In the present case, a similar comparison is not possible because (i) the data are too sparse and do reveal neither vertical nor horizontal structure of the fluctuating fields, and (ii) the complicated topography prevents use of a simple analytical model.

The average input of energy from fluctuating winds is estimated almost an order of magnitude less than potential energy conversion. This result is somewhat ironical as the question of wind generation was one of the main motivations to launch this experiment. Our tentative conclusion is that over most of the time the observed eddies are generated by instability of the polar front. Only occasionally, during the passage of strong atmospheric cyclones (MEINCKE, 1975), wind generation is likely to play the dominant role.

Table 1 - General information on time series obtained at position MONA 1 and MONA 3

Parameter	MONA 1	MONA 3
Position	60°35'N 05°09'W	63°11'N 09°02'W
Bottom depth (m)	947	534
Instrum. depth (m)	896	517
Rec. interval (h)	1	1
Rec. start. (GMT)	JUN 8,75,00	JUN 8, 75,00
Rec. stop (GMT)	FEB 16,76,00	JUN 13,76,00
*Mean speed (cm s ⁻¹)	1.6	1.8
*Mean direction (degr.)	105	32
*Mean temperature (°C)	-	0.68
Eddy kinetic energy (cm ² s ⁻²)	418	584

* From low-passed time series, half-power-period 30 hours, 167 filter weights.

Table 2 - Ratio of major to minor principal axis of current ellipse and orientation of major axis counter-clockwise from east

Period {d}	MONA 1		MONA 3	
	Axis ratio	Direction {°}	Axis ratio	Direction {°}
43	7.0	40	4.5	14
21	6.8	40	3.2	9
14	6.1	40	2.9	18
9.5	6.8	39	4.4	25
6.6	6.2	40	1.8	9
4.7	3.8	38	1.8	38
3.4	3.1	20	2.2	57
2.5	2.6	18	1.7	-5
1.9	2.9	33	2.0	17
1.4	2.3	17	1.3	33
1.1	5.1	22	2.3	-2
.83	2.3	5	1.5	6
.63	1.4	0	1.1	32
.48	14.2	9	5.2	22

FIGURE LEGENDS

- Figure 1 - Bathymetry of the Southeastern Iceland-Faroe ridge and the Faroe Shetland channel with locations of moorings MONA 1 and MONA 3.
- Figure 2 - Sections of temperature based on CTD-measurements in June 1977 by RV Poseidon (after MEINCKE, 1978). Orientation of sections indicated in Figure 1, mooring positions marked.
- Figure 3 - Portion from the time series of temperature and current components (u_1 , east, u_2 north) at position MONA 3.
- Figure 4 - Autospectra of twice the horizontal kinetic energy at both stations.
- Figure 5 - Coherence and phase difference of NE current component between stations MONA 3 and MONA 1. Error bars indicate 95 % confidence interval. Shaded area in coherence diagram indicates 95 %-range of coherence estimate if true coherence is zero.
- Figure 6 - Ratio anticlockwise over clockwise energy for both stations, with 95 % confidence limits.
Full line: Theoretical prediction from eq. (3)
Dashed line: Prediction from eq. (5), with $\lambda^{-1} = 1.5$ h.
- Figure 7 - Values $\lambda(\omega)$ which make observed and predicted E_+/E_- identical at MONA 3. Dashed lines are $\lambda=f$ and $\lambda=\omega$, respectively, for comparison of terms in (4).
- Figure 8 - Coherence and phase difference between rotary current components at both stations. Phase positive if anticlockwise component leads.
- Figure 9 - Full line: Observed temperature spectrum at MONA 3.
Dashed line: Theoretical prediction from eq. (19).
- Figure 10 - Cospectrum between temperature and NNE current at MONA 3.
- Figure 11 - Coherence between temperature and current vs. current direction for various frequency bands. Scale of abscissae applies to 43 d period. Following curves are shifted upwards by 0.25 units each.
- Figure 12 - Coherence and phase difference between temperature and 350° current component (full line).
Dashed line is prediction from eq. (21) and (22).

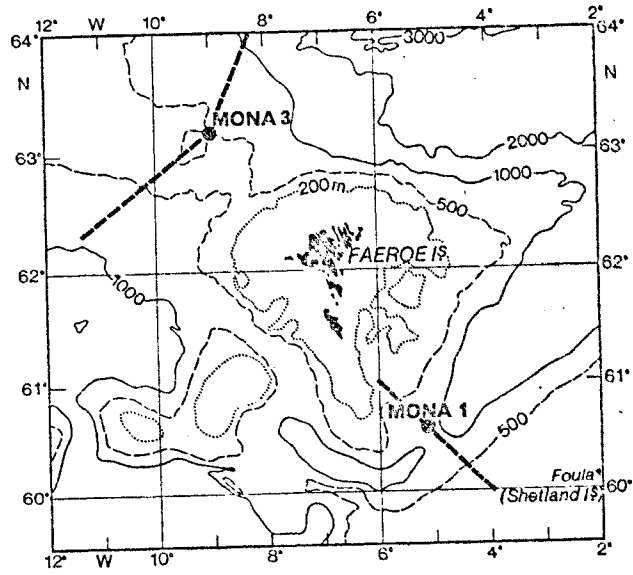


Fig. 1

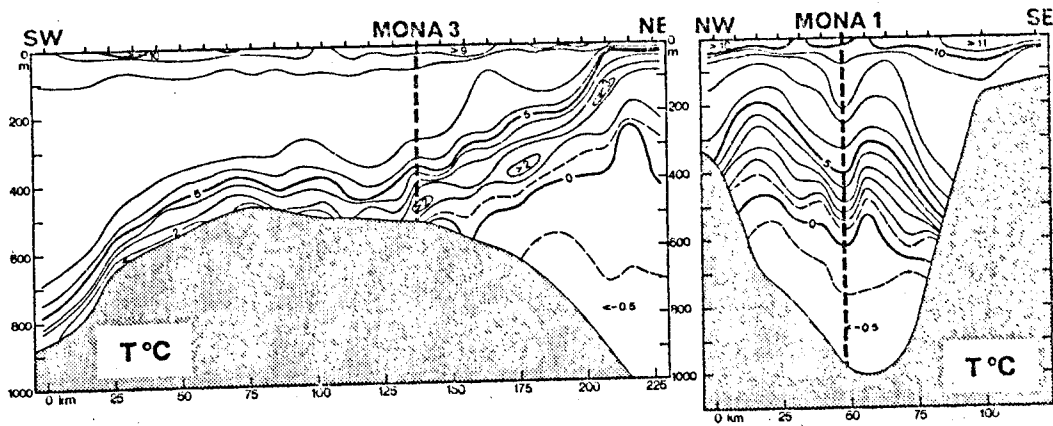


Fig. 2

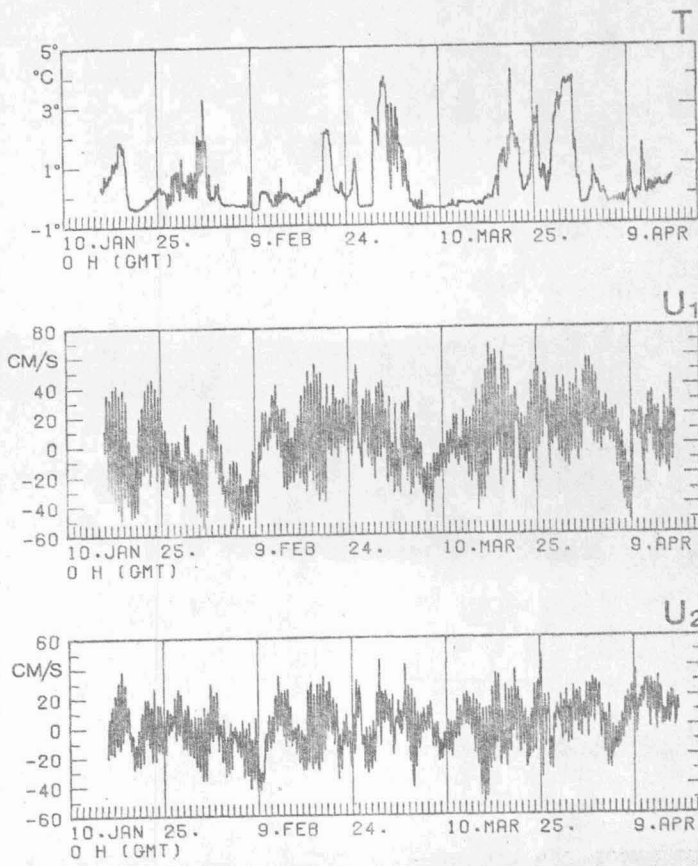


Fig. 3

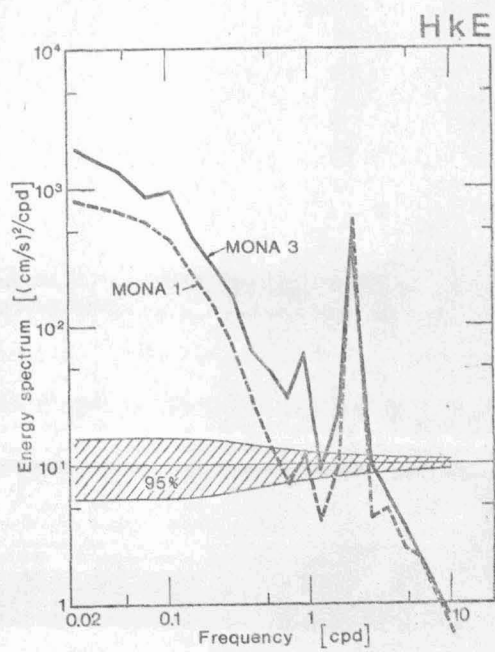


Fig. 4

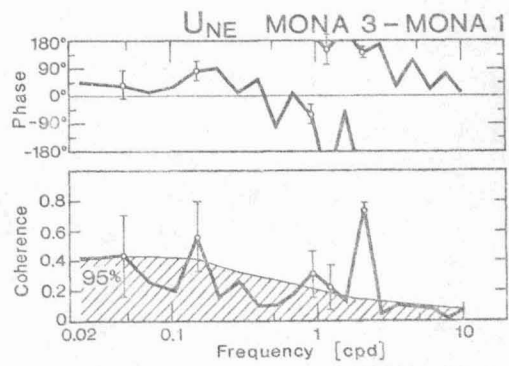


Fig. 5

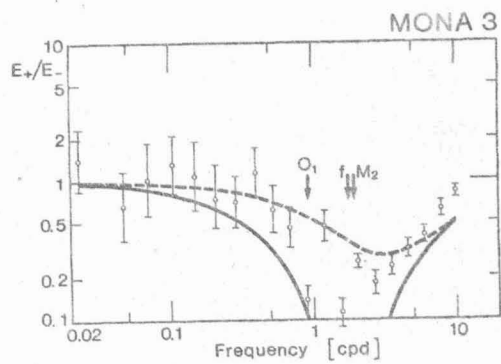
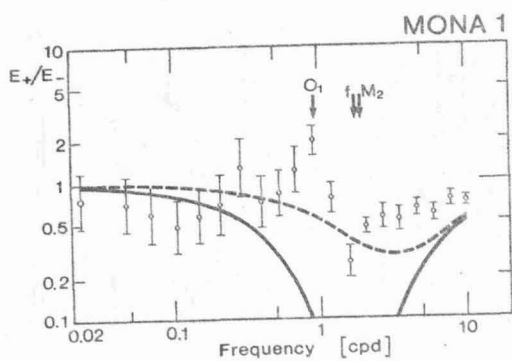


Fig. 6

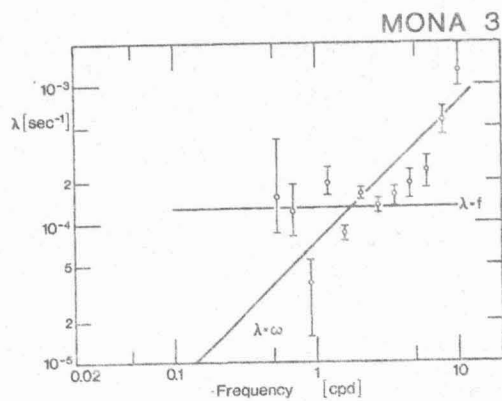


Fig. 7

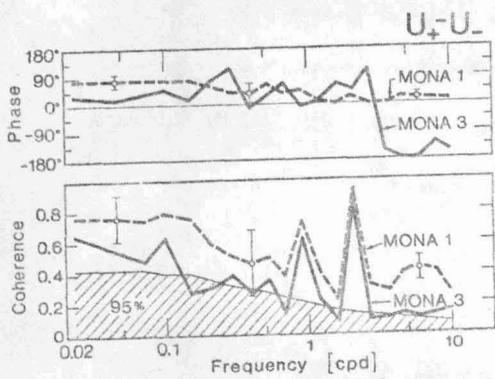


Fig. 8

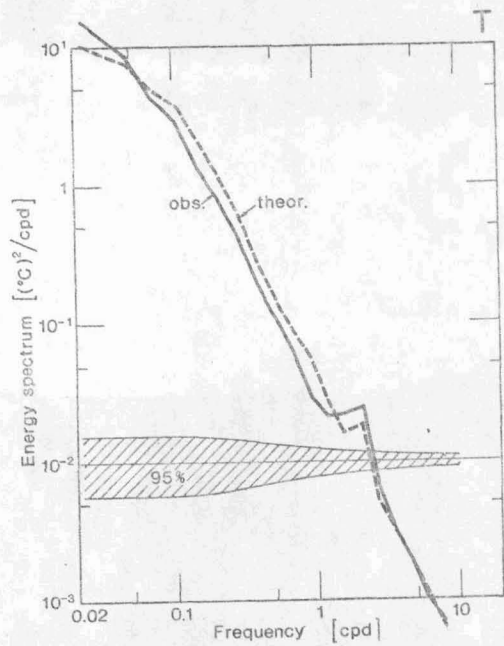


Fig. 9

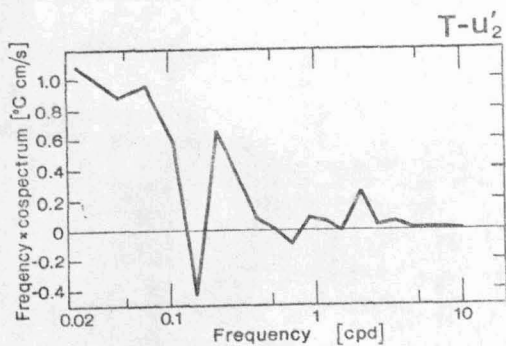


Fig. 10

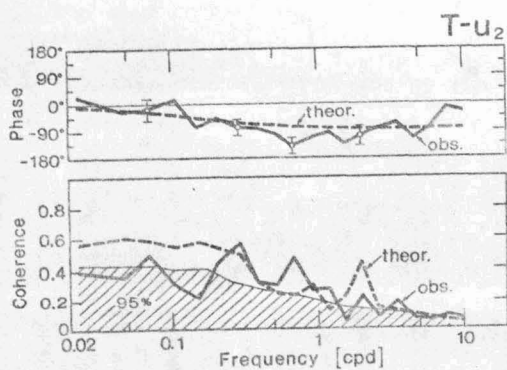


Fig. 12

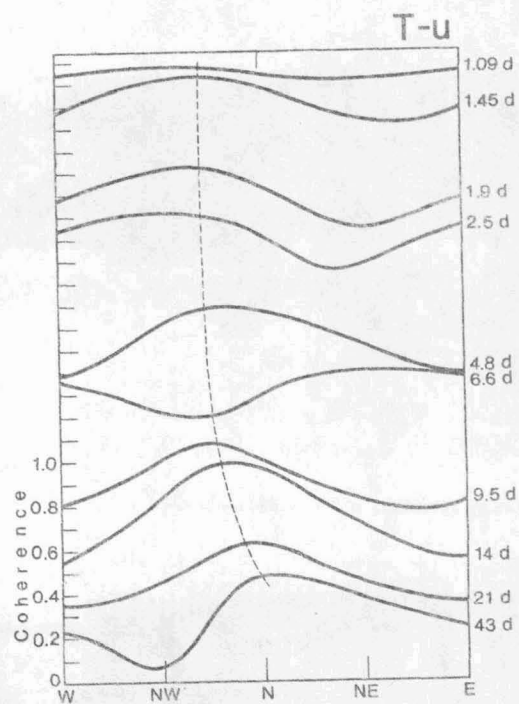


Fig. 11

REFERENCES

- AAGARD, K. and S.-A. MALMBERG, 1978: Low frequency characteristics of the Denmark strait overflow. ICES C.M. 1978/C:47, 22 pp. (unpublished document).
- BRYDEN, H.L., 1979: Poleward heat flux and conversion of available potential energy in Drake Passage. *Journal of Marine Research* 37, 1-22
- FLEISCHER, U., F. HOLZKAMM, K. VOLLBRECHT and D. VOPPEL, 1974: Die Struktur des Island-Farøer Rückens aus geographischen Messungen. *Deutsche Hydrographische Zeitschrift*, 27, 97-113
- FOFONOFF, N.P., 1969: Spectral characteristics of internal waves in the ocean. *Deep-Sea Research* 16 (Suppl.), 58-71.
- GONELLA, J., 1972: A rotary-component method for analyzing meteorological and oceanographic vector time series. *Deep-Sea Research* 19, 833-846.
- HANSEN, B. and J. MEINCKE, 1979: Eddies and meanders in the Iceland-Farøe Ridge Area. *Deep-Sea Research* 26A, 1067-1082.
- KNUDSEN, M., 1899: Hydrography. The Danish Ingolf-Expedition, 1(2), 23-161.
**)
- KOLTERMANN, K.P., 1978: The tidal current constituents during "Overflow '73" ICES C.M. 1978/C:8, 12 pp. (unpublished document).
- LORENZ, E.N., 1967: The nature and theory of the general circulation of the atmosphere. World Meteorological Organization, Geneva, 161 pp.
- MARTIN, J.H.A., 1966: The bottom waters of the Farøe-Shetland channel. In: *Some Contemporary Studies in Marine Sciences* (Barnes, ed., George Allen and Unwin Ltd., London), 469-478.
- MEINCKE, J., 1975: Evidence for atmospheric forcing of Arctic water overflow - events. ICES C.M. 1975/C:29, 13 pp. (unpublished document).
- **)
- KOLTERMANN, K.P., J. MEINCKE and T. MÜLLER, 1976: Overflow '73 - Data Report 'Meteor' and 'Meerkatze'. *Berichte des Instituts f. Meereskunde*, 23, 88 pp.

- MEINCKE, J., 1976: Coupling between bottom currents and weather pattern on the Iceland-Faroe ridge. ICES C.M. 1976/C:30, 8 pp. (unpublished document).
- MEINCKE, J., 1978: On the distribution of low salinity intermediate waters around the Faroes. Deutsche Hydrographische Zeitschrift, 31 (2), 50-64.
- MEINCKE, J. and T. KVINGE, 1978: On the atmospheric forcing of overflow-events. ICES, C.M. 1978/C:9, 10 pp. (unpublished document).
- MÜLLER, P. and G. SIEDLER, 1976: Consistency relations for internal waves. Deep-Sea Research 23, 613-628.
- MYSAK, L.A. and F. SCHOTT, 1977: Evidence for baroclinic instability of the Norwegian current. Journal of Geophysical Research 82, 2087-2095.
- PEDLOSKY, J., 1979: Geophysical Fluid Dynamics. Springer-Verlag, New York, 624 pp.
- PHILLIPS, O.M., 1971: On spectra measured on an undulating layered medium. Journal of Physical Oceanography, 1, 1-64.
- ROSS, C.K., 1976: Transport of overflow water through Denmark Strait. ICES C.M. 1976/C:16, 9 pp. (unpublished document).
- SMITH, P.C., 1976: Baroclinic instability in the Denmark Strait overflow. Journal of Physical Oceanography, 6 (3), 355-371.
- WILLEBRAND, J., P. MÜLLER and D.J. OLBERS, 1977: Inverse analysis of the trimooored internal wave experiment (IWEX). Berichte des Instituts für Meereskunde, 20a,b.
- WILLEBRAND, J., S.G.H. PHILANDER and R.C. PACANOWSKI, 1980: The oceanic response to large-scale atmospheric disturbances. Journal of Physical Oceanography (in press).
- WILLEBRAND, J. and J. MEINCKE, 1980: Statistical analysis of fluctuations in the Iceland-Scotland frontal zone. Deep-Sea Research (in press).